The potential for photovoltaic-powered pumped-hydro systems to reduce emissions, costs, and energy insecurity in rural China

Yang, Z.; Sun, G.; Behrens, P.A.; Ostergaard, P.A.; Egusquiza, M.; Egusquiza, E.; ... ; Patelli, E.

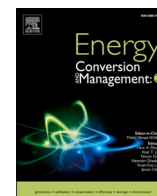**Note:** To cite this publication please use the final published version (if applicable).

Check for updates

The potential for photovoltaic-powered pumped-hydro systems to reduce emissions, costs, and energy insecurity in rural China

Zongru Yang [a,b], Guoxiu Sun [a,b], Paul Behrens [c,d], Poul Alberg Østergaard [e], Mònica Egusquiza [f], Eduard Egusquiza [f], Beibei Xu [a,b,g,h,*], Diyi Chen [a,b], Edoardo Patelli [i]

[a] Key Laboratory of Agricultural Soil and Water Engineering in Arid and Semiarid Areas, Ministry of Education, Northwest A & F University, Shaanxi Yangling 712100, PR China
[b] Institute of Water Resources and Hydropower Research, Northwest A&F University, Shaanxi Yangling 712100, PR China
[c] Institute of Environmental Sciences (CML), Leiden University, 2333 CC Leiden, the Netherlands
[d] Leiden University College The Hague, Leiden University, 2595 DG The Hague, the Netherlands
[e] Department of Planning, Aalborg University, Rendsburggade 14, 9000 Aalborg, Denmark
[f] Center for Industrial Diagnostics (CDIF), Polytechnic University of Catalonia (UPC), Barcelona, Spain
[g] State Key Laboratory of Eco-hydraulics in Northwest Arid Region, Xi'an University of Technology, Xi'an 71065, PR China
[h] Powerchina Northwest Engineering Corporation Limited, Limited, Xi'an 710065, PR China
[i] Centre for Intelligent Infrastructure, Department of Civil and Environmental Engineering, University of Strathclyde, United Kingdom

ARTICLE INFO

ABSTRACT

Homes in rural China often have access to water wells for domestic and agricultural use. Given the significant difference in height between the well water and the roof of the house, such an arrangement could be used as a solar-powered pumped-hydro energy generation system. These systems could both limit increases in carbon emissions from coal-powered electricity while alleviating energy insecurity, while providing significant savings to households. The potential for these systems in rural regions across Shaanxi province is investigated by assessing eight key environmental and socioeconomic indicators. The find is that positive impacts across almost all indicators with generally rapid investment payback periods of 6.4–8.1 years, annual net income increases of 314.2 CNY −541.6 CNY per year per household. This research laid a theoretical foundation for the promotion of PV-PH system in Shaanxi Province.

Introduction

While non-fossil energy in China has grown rapidly in recent years, accounting for 25% of primary energy consumption with an installed capacity of 1200 GW [1], China has announced targets to reduce carbon dioxide emissions per unit of GDP to below 65% by 2030 (on a 2005 baseline). At the same time, there are many challenges in providing low-carbon energy to rural regions of China as they continue to increase their consumption. Balancing emission reductions and costs while improving the security of energy supply will be a key issue for rural policy makers. The National Bureau of Rural Development implemented a policy for encouraging solar photovoltaic (PV) electricity generation along with incentives for improved lighting in 2016. However, rural communities still struggle to provide reliable electricity, and storage technologies are needed to ensure reliability and security of supply [2].

There are a number of potential energy storage devices that could be used for providing reliable electricity, including: compressed air [3,4], pumped-hydro, batteries [5,6], flywheels [7,8], and phase change materials [9–11]. However, many of these technologies cannot be used in rural regions, either because they are too expensive or can only be implemented on large, interconnected transmission grids. A techno-economic analysis is presented for the innovative use of existing water infrastructure in rural regions to meet this electricity storage need. This may lower costs while meeting energy generation and storage requirements. As a more rural province with energy access issues, we investigate regions across Shaanxi, a province with an average annual solar insolation of 1505 kWh/m^2/year. Most rural households in Shaanxi Province have wells and many have solar PV already Fig. 1 installed (an example arrangement is shown in Fig. 3). The natural height of the well water and the height of the house provide a height
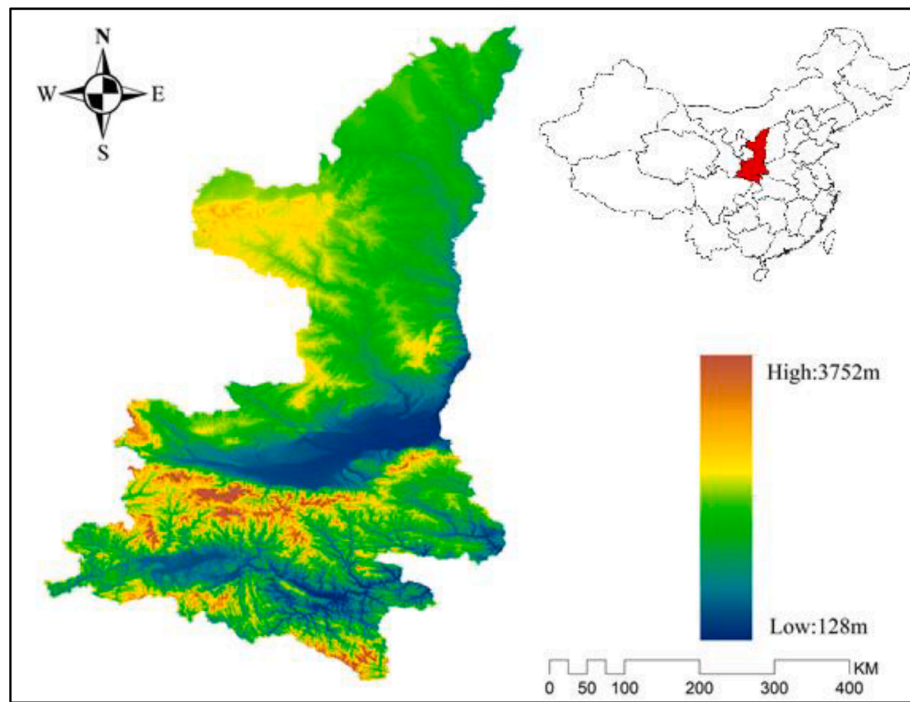

Fig. 1. The location of Shaanxi Province and the elevation across the region.

(*a*)   (*b*)

Fig. 2. (*a*) Solar power generation system and wells on a rural household in Shaanxi Province. (*b*) A solar power generation system on the roof above the well shown in the red rectangle in the photo. (For interpretation of the references to colour in this figure legend, the reader is referred to the web version of this article.) (For interpretation of the references to colour in this figure legend, the reader is referred to the web version of this article.)

difference (termed 'head' in hydropower installations) that can be used to both generate energy from falling water but also allow the pumping of water using solar PV when excess power is available. We term the arrangement here Photovoltaic-powered Pumped-Hydro generator systems (PV-PHs) (see Fig 2).

Flexibility and techno-economic analyses have been conducted for large-scale grid-connected, off-grid, and irrigation-based PV-PH systems. Grid-connected systems have been shown to improve energy security across many studies in both high- and low-income settings [12–14]. Yan et al. [15] found that the levelized cost of energy (L_{CE}) of a PV-PH system in China was much lower than local desulfurized coal electricity. In off-grid settings PV-PH systems have been found to be cheaper than alternatives, for instance Ma et al. [16] found that an off-gird PV-PH system on a remote island off Hong Kong provided reliable, cheap power. There have been several studies investigating energy-the use of PV-PH for irrigation. For example, Yu et al. [17] investigated

the feasibility of irrigating cassava using PV-PH in Guangxi while providing power to the community. Campana et al. [18] also studied the potential ability of PV-PH for grassland irrigation in Qinghai Province. The results show that the food irrigated with photovoltaic water pumping technology is already competitive with imported food. In sum, PV-PH systems have been shown to provide affordable electricity and irrigation services.

Previous work has focused largely on large-scale PV-PH systems. However, smaller systems are more attractive in rural regions due to lower construction costs and small sizes. Some researchers have investigated the potential for micro-PV-PH systems, for example as applied to high-rise residential buildings [19]. Several studies have investigated the potential for micro-PV-PH systems in Africa and India [20–23]. However, few studies evaluate the economic and technical feasibility of a PV-PH installation in rural areas by households and none have analyzed the potential for PV-PH systems using wells. To fill this gap,

Fig. 3. (*a*) a PV-pump used in agricultural irrigation. [18] (*b*) A rendering of a household PV-PH system.
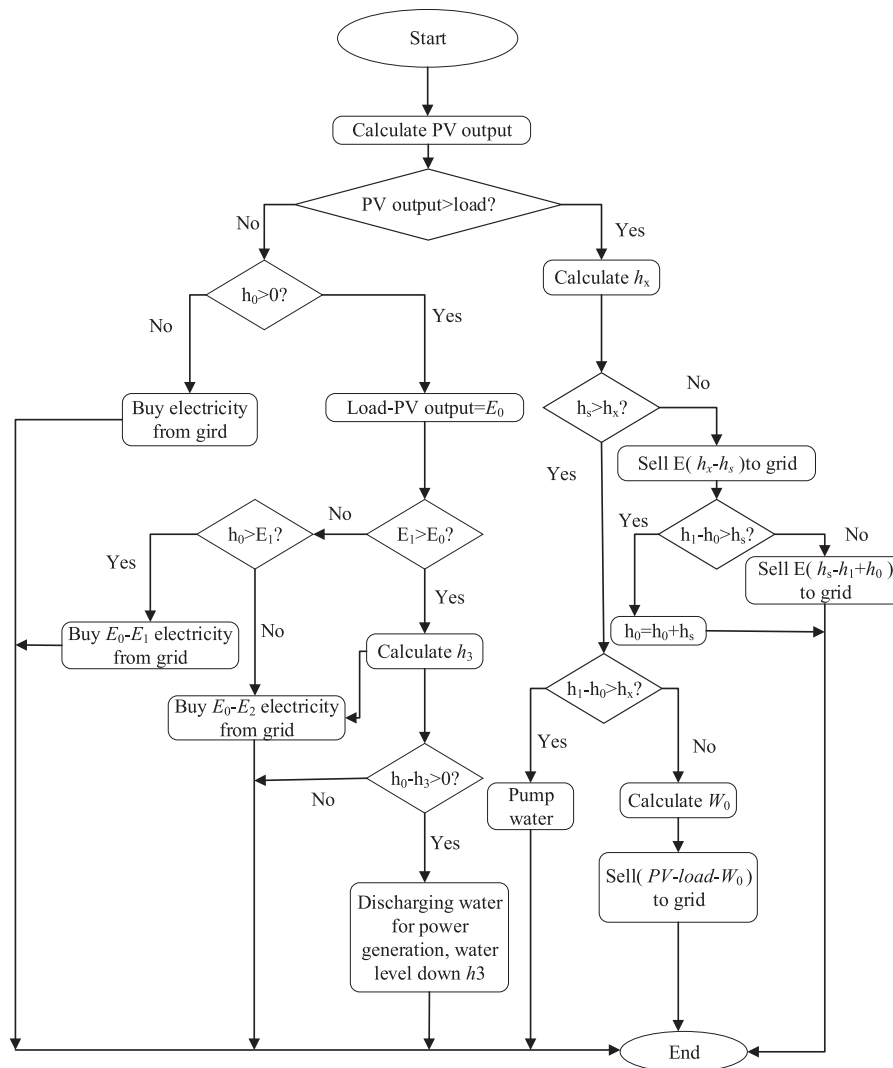
Fig. 4. The operating principles of the photovoltaic-pumped hydropower generating system.

eight techno-economic indicators are investigated for PV-PH systems integrated with family wells and buildings. The analysis is conducted across Shaanxi province, a key area of policy interest for ensuring reliable, affordable energy in rural China.

Method

System layout

Five sub-system elements of the PV-PH storage and generator system

Table 1
The basic parameters of the pump.

Characteristics	Value	Unit
Power	950	W
Suction Head Lift	9	m
Maximum Flow Rate	4.2	m³/h
Top Lift Head	42	m
Size Of Inlet And Outlet	32	mm

Table 3
Basic parameters of hydro generator.

Characteristics	Value	Unit
Power	3000	W
Water flow rate	0.03	m/s
Revolutions Per Minute	1500	r/min
Height Of Water Head	10–25	m
Efficiency	75	%

are modeled by MATLAB: PV modules, DC-DC converter, centrifugal pump, hydropower generator and an upper water tank acting as the energy storage (see Fig. 3 for an example layout (not for hydropower)). The upper water tank releases water when the PV array cannot meet residential demand. Given roof structures, in rural regions, the maximum load of water pressure is 1.5 m [24]. For a conservative estimate to avoid structural loading, a closed, airtight, upper water tank with a height of one meter is assumed in this study. The PV modules are installed on the water tank's upper surface to take full advantage of the roof area. The penstock is arranged perpendicularly to the residential house wall and the inverter is integrated into the PV array. The household buys electricity from the power grid when the system output cannot meet load demand and sells electricity to the power grid when there is a surplus.

The PV-PH system using four operating modes are modeled by MATLAB: pumping water, draining water, selling electricity to the power grid, and buying electricity from the grid. The switching of these modes depends on the output power of the PV array, the power of the generator, the water content of the water tank, and local electricity demand. The key to identifying the different system operation principles is to compare the value between PV outputs and the load demand of the family (see the schematic in Fig. 4).

An optimally-tilted fixed PV array consisting of Jinkosolar Ltd is assumed in this study. Panels with a rated power of 455 W and efficiency 20.89% (model: JKM455M-72HLM-BD, see key parameters in Table 1). The capital cost of the PV array is assumed to be 1.6 CNY/W [25]. The calculation of the electrical output of the PV array follows standard modeling (for full details see the SI). The pump water storage system is composed of pumps, generators, upper water tanks, lower water tanks, and penstock. [19] The pump and generator are considered as one module. The height of the water pumped up in one hour in the upper water tank (in m) is given by:.

$$h_P = \frac{P_{\text{pump}} \times 3.6 \times 10^6}{\rho_{water} \times g \times h_1 \times S} \tag{1}$$

where, P_{pump} is the output power of the pump; ρ_{water} is the water density; g is acceleration under gravity; h_1 is the height between the upper water tank and lower water tank and S is the area of the roof water tank. Some pump parameters are assumed in this study, including the pump has a power of 950 W, suction head lift of 9 m, maximum flow rate of 4.2 m³/h, lift head of 42 m and size of inlet/outlet of 32 mm. If the PV array cannot meet household electricity demand, and if there is water in the upper water tank, then the generator will produce electricity to meet

demand. The output of the generator is determined by the rated output power of the generator and the energy conversion efficiency of the generator. A generator efficiency of 0.75 with a rated output of 3000 W is assumed in this study (the specific model is JET-G17-37 made by KL Ltd).

Generator power is given by:

$$P_{generator} = \frac{0.75 h_2 \rho_{water} g h_1 S}{3.6 \times 10^6} \tag{2}$$

or

$$P_{generator} = P_{rate-output} \tag{3}$$

When the water in the upper water tank cannot generate enough electricity to meet the household load demand in an hour Eq. (5) will be used where h_2 is the water height of the upper water tank and other parameters indicate the same as in Eq. (4). Eq. (6) is used when the water in the upper water tank generates enough electricity to meet household load demand in an hour. In Eq. (6), the $P_{\text{rate-output}}$ is the rated output of the generator of 3000 W. Hydro generator specific parameters as shown in Table 3.

The state of charge for the water tank is reflected by the water level of the upper water tank. If the electricity generated by the solar PV exceeds load demand, the water level in the water tank rises. In the reverse situation, the water in the upper water tank is used to generate electricity and the water level drop if the solar PV does not meet the household load. If the output of the PV array exceeds the load demand of households, then:

$$h_2 = 3.6 \times 10^6 \frac{(P_{PV} - P_{load})}{\rho_{water} g h_1 S} + h_{before} \tag{4}$$

Otherwise:

$$h_2 = h_{before} - 3.6 \times 10^6 \frac{(P_{load} - P_{PV})}{0.75 \rho_{water} g h_1 S} \tag{5}$$

where the h_{before} is the previous hour's water level, and the initial water level is set to zero. P_{load} is the hour household electricity consumption, which is obtained by the dataset of household electricity profile.

Simulation data

Shaanxi is located in central China and consists of ten prefecture-level regions (see SI for full details). Shaanxi experiences a subtropical monsoon climate in the south and a temperate monsoon climate in the north, with sufficient solar radiation and abundant precipitation. In the rural areas of Shaanxi, most households are detached with two or three floors and a yard. Solar radiation data are obtained from SolarGIS. Long term yearly average of direct normal irradiation in Shaanxi Province is shown in Fig. 6 SI 1.2. Load profiles are obtained from public data [26] recording the electricity consumption data of a family in the past year at a minute resolution (which is aggregated to the hourly timestep used here) (see figures in Fig. 5(a) SI 1.2 and Fig. 5(b) SI 1.2 for more details).

Optimization algorithm

The size of the system must be optimized for households. Different optimization methods, such as intuitive [27,28], analytical iterative [29], and Numerical [30–32], artificial intelligence based [16,23,33,34] methods have been used to size different energy systems. Among artificial intelligence method, GA [16,34] and PSO [23,33] algorithms are the most widely used. Compared with the GA algorithm, the PSO algorithm has a faster convergence speed, but the PSO algorithm is easier to fall into a local optimal solution than the GA, and the algorithm is also
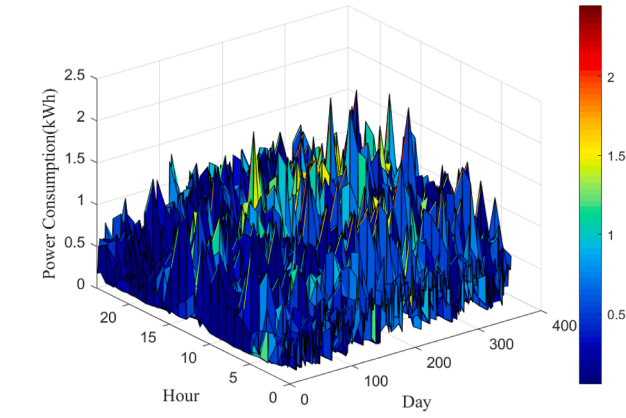
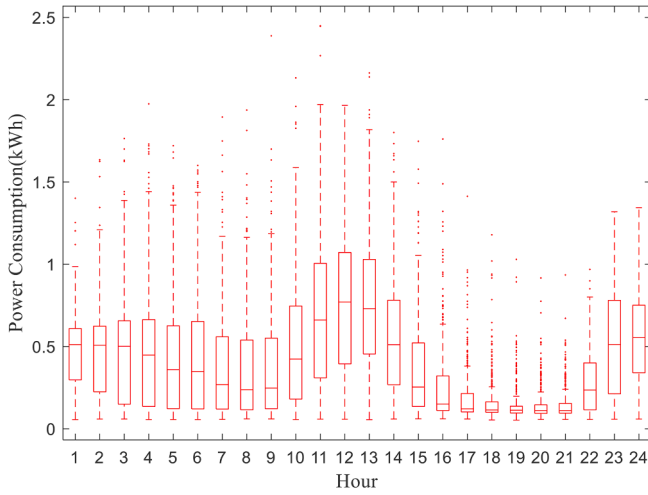(*a*) Family electric load in one year of the Load profile.

Fig. 7. Flowchart of the system-sizing optimization.

unstable. Therefore, Genetic Algorithm (GA) is used to solve this multi-objective optimization problem. The optimal size of the PV-PH system is transformed into a multi-objective optimization problem based on two objective functions: the Payback Period (PBP) and Hours Sold to the Grid (HSG). A smaller indicator of PBP means a quicker break-even period on the investment for the family and a higher H_{SG} results in greater income due to more hours of generation sold to the grid. Increasing the value of H_{SG} generally requires more solar photovoltaic panels. However, using solar panels with higher conversion efficiency or installing more solar panels leads to increased costs and further increases the payback period P_{BP} so the two objective functions are inversely related. The relationship between the two is optimized using a genetic algorithm, as shown in Fig. 7. GA include three basic genetic operators: selection, crossover and mutation.

Selection

The process of selecting superior individuals from the group and weeding out inferior individuals is called selection. Roulette wheel selection is the simplest and most used selection method. In this method, the selection probability of each individual is proportional to its fitness. Suppose the population size is *n,* and the fitness of individual *i* is f_i. The probability of *i* being selected is:

$$p_i = f_i / \sum_{j=1}^{n} f_i \tag{9}$$

Obviously, the probability reflects the proportion of the fitness of *i* in the total fitness of the entire group. The greater the fitness of an individual, the higher the probability of being selected, and vice versa.

Crossover

Crossover is to select two individuals from the population to cross over to obtain a new individual with a certain probability. Real number coding is used in the article, so the real number crossover method is used for crossover. The crossover operation method of the mth chromosome am and the nth chromosome an at the i-th position is as follows, where b is a random number between [0,1]

$$\begin{cases} a_{mi} = a_{mi}(1-b) + a_{ni}b \\ a_{ni} = a_{ni}(1-b) + alb \end{cases} \tag{10}$$

Mutations

Mutation is the process of randomly selecting an individual from the population to mutate with a certain probability to obtain a new individual. For example, to mutate the nth gene of the mth individual, the method is as follows

$$a_{mn} = \begin{cases} a_{mn} + (a_{mn} - a_{max}) \times f(g), & r > 0.5 \\ a_{mn} + (a_{min} - a_{mn}) \times f(g), & r \leqslant 0.5 \end{cases} \tag{11}$$

where the upper bound of the gene a_{mn} is a_{max}, $f(g) = r_2(1 - g/G_{max})$, *g* is the current iteration number, G_{max} is the maximum evolution number, *r* is a random number between [0,1], r_2 is a random number.

Termination condition

When the fitness of the optimal individual reaches a given threshold, or the fitness of the optimal individual and the group fitness no longer rise, or the number of iterations reaches the preset number of generations, the algorithm terminates.

In this research, three key parameters are selected as decision variables: the number of PV arrays, the size of the water tank, the height of the head. According to our previous assumption that the height of the water tank is 1 m, the size of the water tank is transformed into the area of the water tank. Optimize these three decision variables to find the optimal size of the PV-PHS system. The search area of the decision variables is [0,30] for both numbers of PV array and the height of the head and [80,120] for the area of the water tank. Meanwhile, after making multiple attempts to optimization the program, the number of generations is set to 50 to ensure the stability of the solution. The recommended values of the mutation factor and crossover rate are 0.8 and 0.2, respectively.

Here, three key parameters are selected as decision variables (upon which crossover and mutation can happen): the number of PV arrays, the size of the water tank, the height of the head. According to our previous assumption that the height of the water tank is 1 m, the size of the water tank is transformed into the area of the water tank. Optimizing these three decision variables results in the optimal size of the overall PV-PH system. The search area of the decision variables is between 0 and 30 PV panels. Between 80 m and 120 m for the head height (height between well water and roof) and X to Y for the area of the water tank. The algorithm is run for 50 generations. The recommended values of the mutation factor and crossover rate are 0.8 and 0.2, respectively. The calculated result using genetic algorithm is composed of many optimal solutions for different roof sizes and well depths. The set of these optimal solutions is the Pareto front [35]. From a practical engineering point of view, the Pareto front has many solutions (there are 100 initial populations in simulations, and 35 sets of optimal solutions). However, it is necessary to select the most suitable model parameters to promote the PV-PH system. Here one solution is selected by MCDM method to evaluate the system cost, emission and energy security impacts.

5

Table 5
The initial cost of the PV-PH system in 2021.

Physical meaning	Cost	Unit
PV array	1.6	W/CNY
	728	array/CNY
Pump machine	418	CNY
Penstock [37]	150	CNY
Control center [38]	1258	CNY
Digging a well [39]	120	m/CNY
Reservoir [19]	110	m³/CNY

Economic and technical evaluation indicators

Eight indicators are used to evaluate PV-PH systems including 4 economic indicators and 4 technical indicators. The 4 economic indicators include: P_{BP}, non-discounted payback period, I_{RR}, internal rate of return, L_{OE}, levelized cost of energy, and N_M Net margin. The payback period in capital budgeting refers to the time required to recoup the funds expended in an investment or to reach break-even. A shorter payback is better for the investor. this is computed as a combination of capital costs:

where C_{PV} is the cost of PV panels; C_{pump} is the cost of pump; $C_{generator}$ is the cost of generator; $C_{penstock}$ is the cost of penstock; $C_{water-tank}$ is the cost of water-tank; $C_{control-centre}$ is the cost of control center. $C_{maintenance-cost}$ is the cost of maintenance. C_{GS} is the government subsidies, which is 1CNY/W in Shaanxi province [36]; C_{AR} is the Annual revenue (see Table 5).

The internal rate of return discounts the costs in the payback time by inflation and is computed for when:

$$0 = \sum_{t=1}^{T} \frac{C_t}{(1 + I_{RR})^t} - C_0 \tag{13}$$

where, the period t is set to 25 years, the usual guarantee length of PV-PH systems. C_t is the net cash inflow during the period t. C_0 is the initial investment cost. The L_{CE} gives the average net present cost of electricity generation for a generating plant over its lifetime. It is calculated as the ratio between all the discounted costs over the lifetime of an electricity generating plant divided by a discounted sum of the actual energy amounts delivered [2]:

$$L_{CE} = \frac{C_{ini} - C_{sub} + \sum_{t=1}^{n=25} C_{mai}}{\sum_{t=1}^{n=25} E_t} \tag{14}$$

$$P_{BP} = \frac{C_{PV} + C_{pump} + C_{generator} + C_{penstock} + C_{water-bank} + C_{control-center} + C_{maintenance-cost} - C_{GS}}{C_{AR}} \tag{12}$$

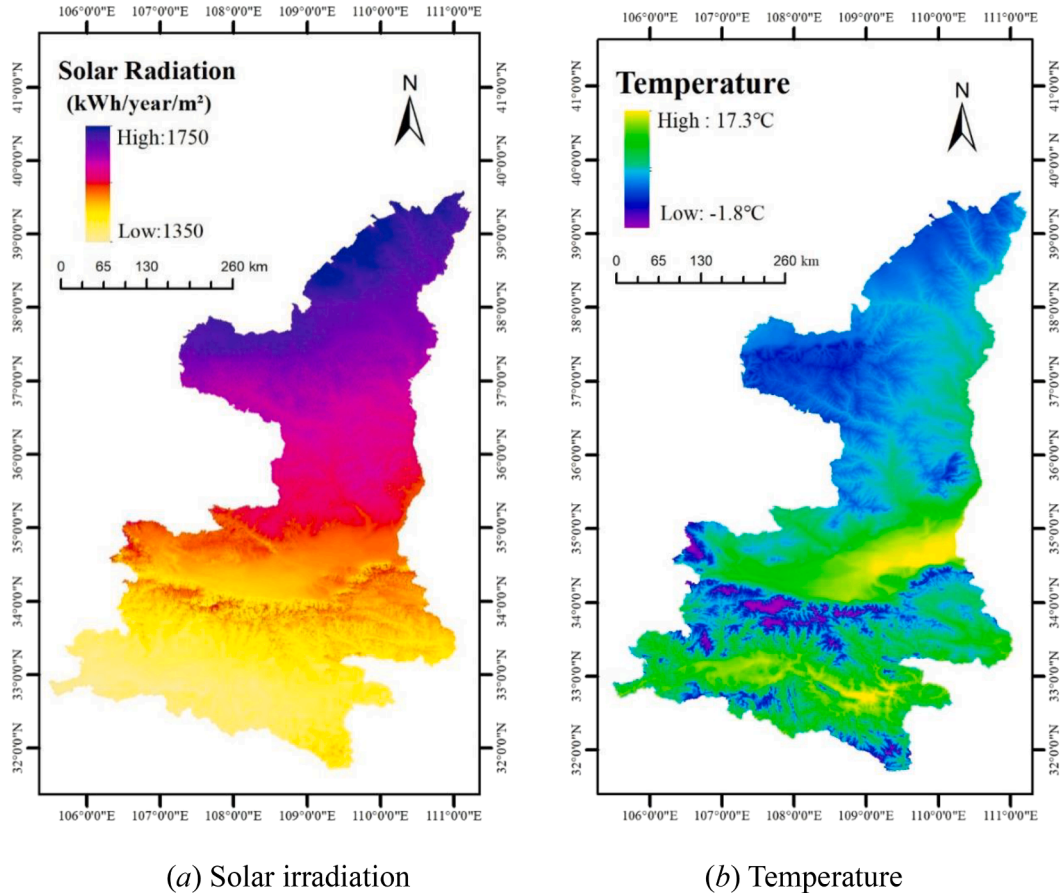(*a*) Solar irradiation

(*b*) Temperature

Fig. 8. Pareto frontier of the Genetic algorithm in 10 prefecture-level cities in Shaanxi Province. See SI for the two letter city acronyms.

Table 6

Scenario definition of the PV-PH system. S_{WT}, H_{TH}, and P_{VN} refers to the size of the water tank, the height of the head, and PV Number.

City	Scenario 1			Scenario 2			Scenario 3		
	S_{WT}	H_{TH}	P_{VN}	S_{WT}	H_{TH}	P_{VN}	S_{WT}	H_{TH}	P_{VN}
XA	120	30	20	120	30	28	120	30	15
YL	120	30	20	120	30	28	120	30	15
WN	120	30	21	120	30	28	120	30	30
YA	120	30	19	120	30	27	120	30	25
XY	120	30	21	120	30	30	120	30	28
SL	119	30	21	120	30	30	119	29	18
AK	120	30	20	120	30	28	120	30	15
HZ	120	30	20	120	30	15	119	30	20
BJ	119	30	19	120	30	25	116	29	15
TC	118	30	20	120	30	30	116	30	16

where E_t is the electrical energy produced in the year, assumed to be the same value in every year. C_{mai} is the cost of maintenance for the PV system, set to 0.025 CNY/W/Year [40]. N_M refers to the annual net margin. This indicator can intuitively reflect the situation in which rural residents can benefit from the PV-PH system. The more profits are made, the stronger the residents' willingness to invest. N_M the calculation formula is as follows:

$$N_M = AFG - PEG \tag{15}$$

where AFG is the Annual profit from selling to the grid, PEG is the price of buying electricity from the grid each year. The remaining 4 technical indicators include the amount of time electricity is sold to the grid H_{SG} (in hours), PV output P_{VO} (in Wh), the number of hours when electricity is purchased from the grid B_{FG} (in hours), and the volume of pumped water through a year P_{HSW} (in m³).

Results

Section "Optimization results and energy flow analysis" is about the results of the system optimization and then analyses the load and generation dynamics of the system. Section "Eight indicator map visualization" provide the results of the 8 indicators and finally, Section "Sensitivity analysis" is about a sensitivity analysis to explore the influence of system variables on the economic performance of the PV-PS system.

Optimization results and energy flow analysis

The optimal solution for the system arrangement is shown in Fig. 8, balancing the payback period and hours of exported solar to the grid. The payback period is between 6 and 9 years across province regions. The payback period across all regions is much lower than estimates for India using PV-PH at 15 years [23]. The distribution of H_{SG} is very broad, from 500 to 1200 h. When H_{SG} is above 1000 h, electricity is sold to the power grid for profit about one-fifth of the year. Fig. 10.

The energy flows for each prefecture are given in Table 6. The specific results of the energy flow of the PV-PH system within a year are shown in Figs. 9 and 10. Specific size parameters are shown in Table 6. We choose the selected point as Scenario 1, the upper right in Pareto curve as Scenario 2 and the bottom left point as Scenario 3.

As shown in Fig. 9(a), 42%–45% of electricity is directly from the solar photovoltaic panel, 16%–23% is purchased from the power, and 34%–38% is from the water tank. The PV-PH system meets approximately 80% of the household's load. For the PV output, about 14%–15% of electricity generated by photovoltaic panels is lost. This is due to the friction loss between mechanical devices in the process of pumping water and discharging water. About 33%–36% of electricity is directly supplied to the family load. 27%–30% of electricity is discharged to the pumped storage of the water tank, and about 19%−26% of electricity is sold to the power grid. So this part of the energy flowing into the PV-PH system has a greater loss, and the proportion of this part of energy is
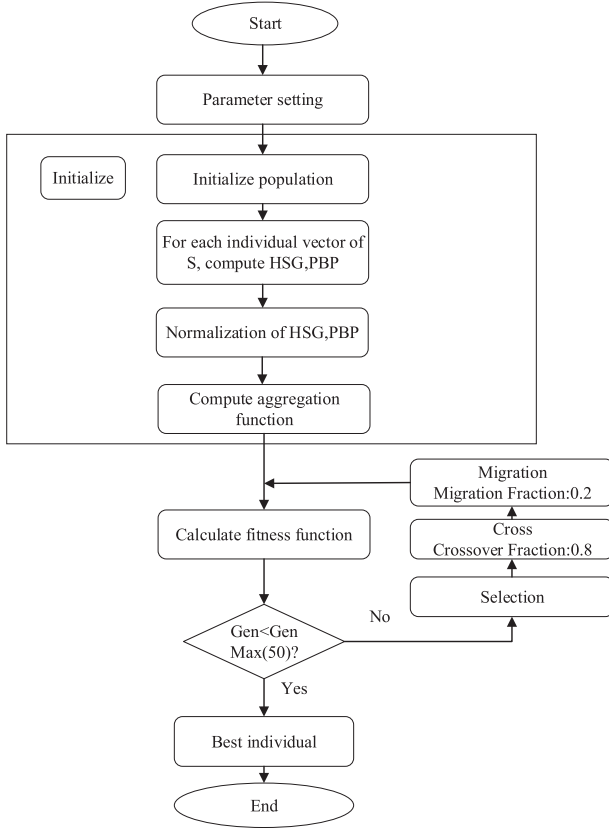

Fig. 9. Energy flow of the PV-PH system within a year in three typical scenarios. (*a*) Scenario 1: Energy flow of the load consumption (*b*) Scenario 1: Energy flow of the PV system (*c*) Scenario 2: Energy flow of the load consumption (*d*) Scenario 2: Energy flow of the PV system (*e*) Scenario 3: Energy flow of the load consumption (*f*) Scenario 3: Energy flow of the PV system.
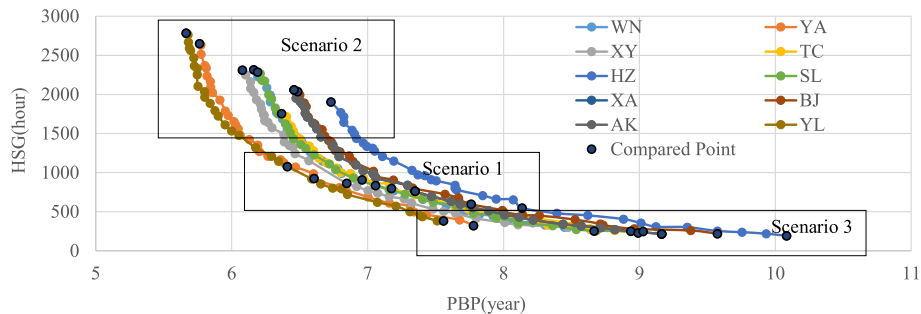
Fig. 10. Energy flow of the photovoltaic-pumped hydropower generating system in different cities.

(a)

(b)

(c)

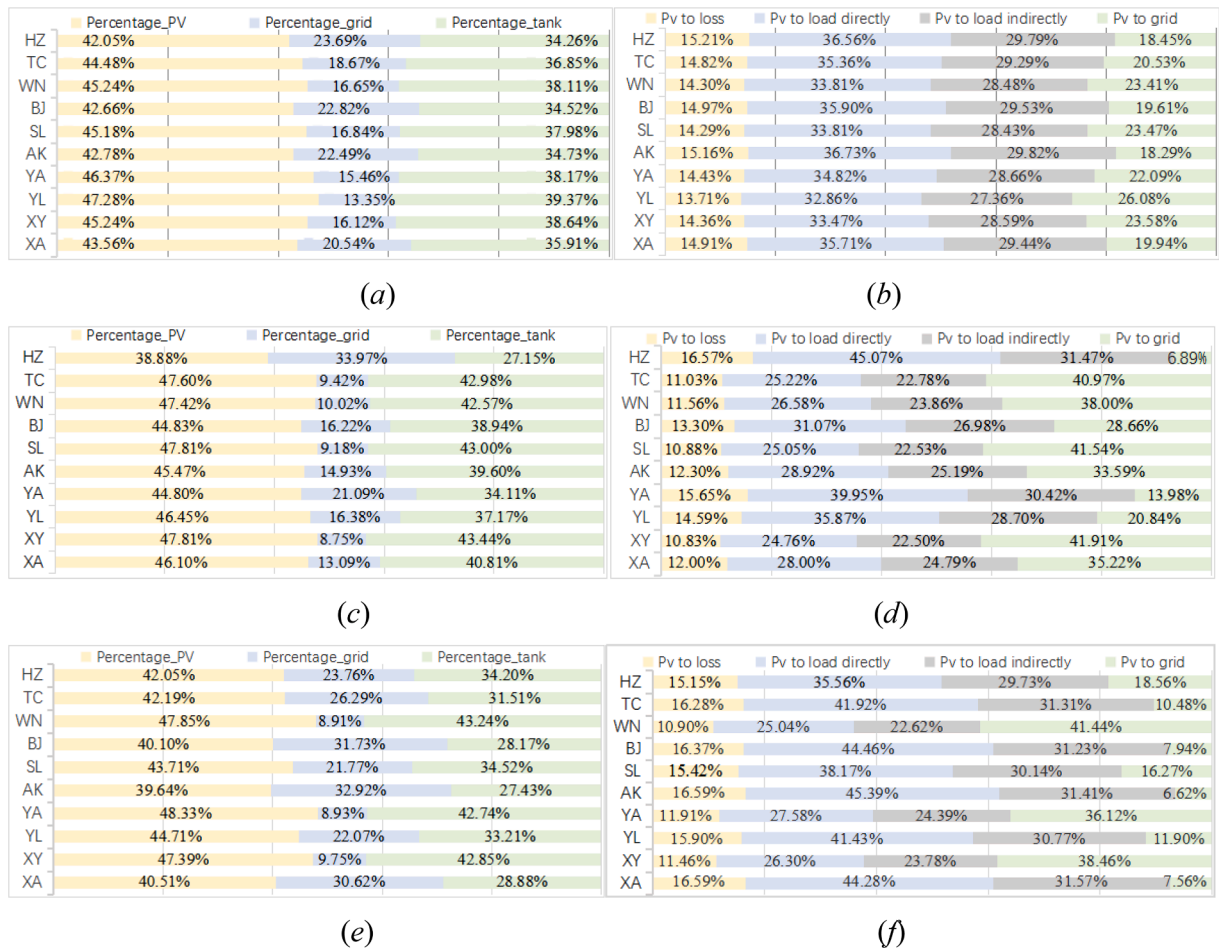(d)

(e)

(f)

Fig. 11. Techno-economic Evaluation of a PV-PH System. (*a*) The payback period (P_{BP}) (*b*) The internal rate of return (I_{RR}) (*c*) The Levelized cost of Energy (L_{CE}) (*d*) The net margin (N_M) (*e*) The hours sold to grid (H_{SG}) (*f*) The PV output (P_{VO}) (*g*) The hours buy from to the grid (B_{FG}) (*h*) The PHS pump water (P_{HSW}).

(*a*) YuLin

(*b*) YanAn

(*c*) HanZhong

(*d*) Baoji
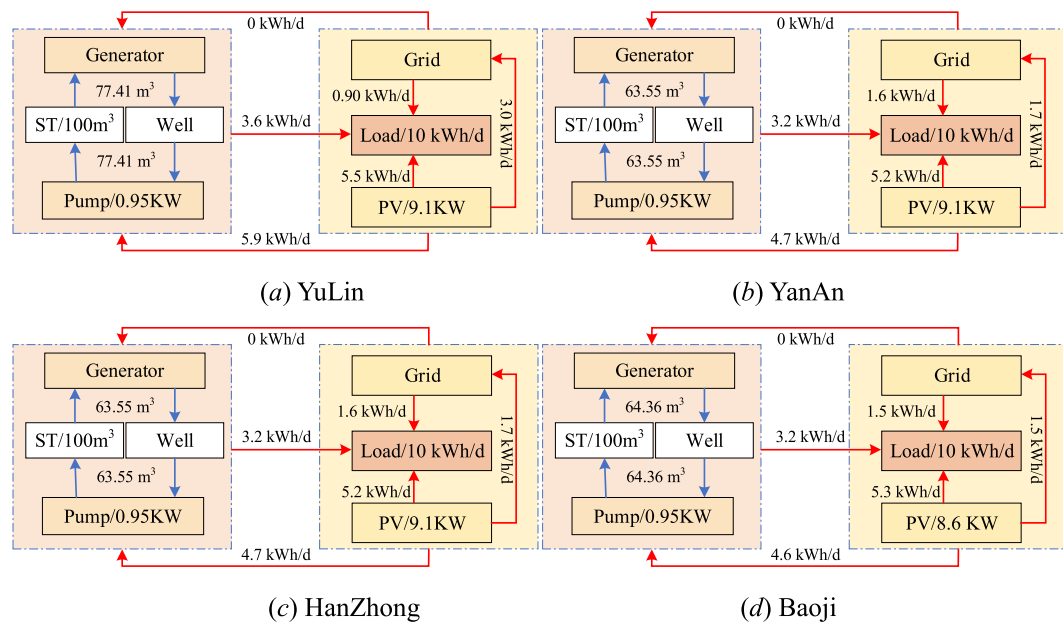
Fig. 12. The relationship between the eight indicators for ten prefecture-level cities in Shaanxi of China. (*a*) Technical Indicators, including the hour sold to the grid (H_{SG}), Indicator of PV output (P_{VO}), Indicator of Buy from the grid (B_{FG}), Indicator of Pumped capacity (P_{HSW}) (*b*) Economic Indicators, including the internal rate of return (I_{RR}), the levelized cost of energy (L_{CE}), the payback period (P_{BP}), and Indicator of Net Margin (N_M).

Fig. 13. Correlation analysis of four evaluation indexes.

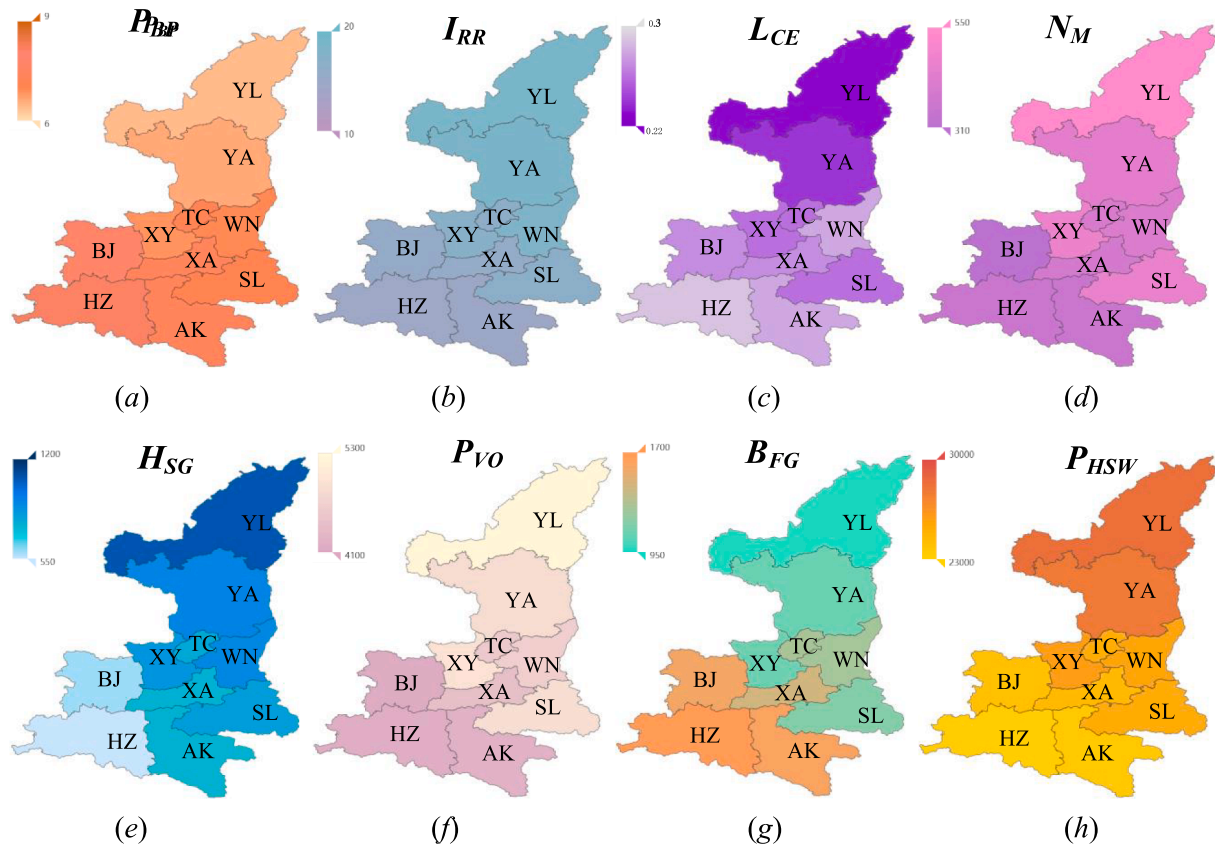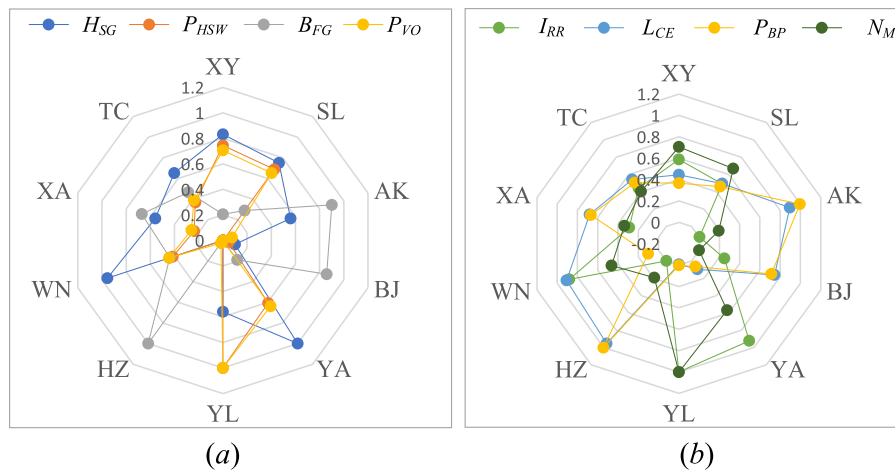**Fig. 14.** Sensitivity analysis of the PV output, power load, water height, and electricity price on indicators of the hour sold to the grid (H_{SG}), the payback period (P_{BP}), the internal rate of return (I_{RR}), and the levelized cost of energy (L_{CE}).

reduced as much as possible for households. For scenarios 2 and scenario 3, the energy flow of the PV-PH system changes greatly. For example, in scenario 2, 33.97% of the load demand of HZ is met by the power grid, while only 8.75% of the load demand of XY is met by the power grid. The same trend is also shown in the energy flow chart of photovoltaic. For example, in scenario 2, only 6.89% of the electricity generated by photovoltaic is sold to the grid at HZ, while the proportion is as high as 41.54% in SL. This reflects that the different size of the PV-PH system has a very significant impact on the energy flow and load demand of the family.

Eight indicator map visualization

There are some economic and technical indicators to reflect the economic and technical feasibility of the system. Lin S. et al. [19] use economic and technical three indicator (self-consumption rate (SCR), self-sufficiency rate (SSR), PBP) to evaluation model. However, this does not fully reflect the economic and technical nature of the system. For example, it is difficult to reflect the relationship between the investment income of the system and the local inflation rate, and it is also difficult to reflect whether the local area can vigorously promote the PV-PH system to replace the local thermal power station. Therefore, more indicators
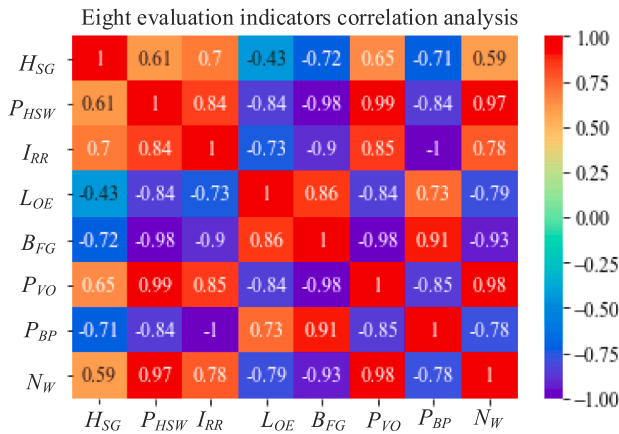
Eight evaluation indicators correlation analysis

Fig. 15. Sensitivity Analysis of Electric Habits about four indicators.

Table 2
The basic parameters of the PV module (Type: JKM455M-72HLM-BD).

Characteristics	Value
Open circuit voltage (V_{oc})	49.76 V
Optimum operating voltage (V_{mp})	41.59 V
Short circuit current (Isc)	11.63 A
Optimum operating current (I_{mp})	10.94 A
Maximum power at STC(P_{max})	455 W

Table 4
The geographical location of 10 prefecture-level cities in Shaanxi Province.

City	Latitude	Longitude	Altitude
XY	34.11	107.38	390
SL	33.88	109.96	700
AK	32.7	109.02	280
BJ	33.35	106.18	590
YA	36.59	109.49	970
YL	38.8	109.77	1150
HZ	32.08	105.30	510
WN	34.13	108.5	380
XA	33.42	107.4	420
TC	35.34	109.29	680

are try to used to evaluate the economic and technical feasibility of the system. In this subsection, eight indicators, including four economic indicators: the payback period (P_{BP}), the internal rate of return (I_{RR}), and the levelized cost of energy (L_{CE}), Net Margin (N_M), and four technical indicators: the hour sold to the grid (H_{SG}), PV output (P_{VO}), Buy from the grid (B_{FG}), the pumped water (P_{HSW}) are used to evaluate the techno-economic performance of the PV-PH in Shaanxi Province. The obtained results are shown in Fig. 11.

As shown in Fig. 11, the payback period in Shaanxi is among 6–9 years and this PBP within the acceptable range. The lowest is 14.5% in HZ and the highest is 18.85% in YL. This is far higher than the China's average inflation rate (2%–3%) as well as far higher than Bank of China's interest rate (4%–5%), which indicates that this investment is worthwhile. The distribution range of L_{CE} in Shaanxi Province is 0.23 kWh/CNY to 0.29 kWh/CNY, which is lower than the power price of desulfurized coal (0.3545 kWh/CNY) in Shaanxi Province. The N_M is between 300 and 500 yuan, which is a considerable income for a family in Shaanxi. These four economic indicators show that the PV-PHS system in Shaanxi Province has good economic effects and is suitable for promotion in Shaanxi Province. The lowest H_{SG} is 547.09 h in HZ and the highest is 1077.42 h in YL, which means almost one-ninth of a year is

to supply power to the power grid in YL. The lowest P_{VO} is 4176.50 kWh, and the average daily power generation exceeds 10 kWh, which means that the daily power generated by photovoltaic panels exceeds the average daily power consumption of the family. The highest B_{FG} is 1690 h in HZ and the lowest is 953 h in YL. The lower B_{FG} means the PV-PH system the higher the technical feasibility. The highest PHSW is 28253 m³ in YL and the lowest is 23195 m³ in HZ. The more water is pumped, the more energy loss in the system. Four technical indicators show that this PV-PHS system has good technical potential in Shaanxi, and the system is operating in good condition.

To obtain the relationship between the eight indicators, Fig. 13 is plotted to obtain the situation of the eight indicators in the ten typical regions of Shaanxi Province.

From Fig. 12 (a), the indicator H_{SG} varies in different regions. The cities of WN and YA have up to 100%, which are the two regions with the highest hours' number of annual electricity sales in all regions. The P_{HSW} of XY and SL have higher values and little difference, indicating that these two regions have the most water pumped by pumped energy storage devices each year, and pumped energy storage devices also generate more electricity than other regions at night. The P_{VO} of different regions are also different, which is directly related to the climatic conditions of regions. Among them, YL has the most photovoltaic power generation in all regions, followed by XY, SL and YA, but the photovoltaic power generations in AK, HZ and BJ are very low. Because the photovoltaic power generations in these cities are not high, resident households need to buy more electricity from the power grid in order to meet electricity consumption of families, so the indicator BFG in AK, HZ, and BJ is very high. In addition, the photovoltaic power generation is first supplied to pumping water storage devices for pumping water, leading to the indicators P_{VO} and P_{HSW} have a positive connection. Hence, it is seen that the regions with high P_{VO} and P_{HSW} or low P_{VO} and P_{HSW}, which is in line with the expected work effect of this PV-PH system.

From Fig. 12(b), it is seen that there is a big gap between the four indicators in different regions. Among them, YL has the highest value of I_{RR} among the ten cities, indicating that the application of the PV-PH system in this city has the best ability to resist economic risks. At the same time, the indicator PBP has the lowest value among these cities, and N_M has the highest value, indicating that the YL's PV-PH system has the shortest payback period and the highest net income to local residents. L_{CE} represents the cost of electricity per kilowatt-hour of the PV-PH system under the constraints of various external conditions such as light resource conditions and electricity price policies. YL also has the lowest value among these cities, so it is considered that the application of PV-PH system in YL area has very good economic advantages. The four indicators of XY and TC are quite satisfactory, but the performance of XY is better than that of TC. The values of indicators N_M and I_{RR} are higher than that of TC, and L_{CE} and P_{BP} are both lower than TC. The indicators N_M, L_{CE} and P_{BP} for SL are very similar to XY, but its I_{RR} is much lower than that of XY. This indicates that the PV-PH system in SL is far less able to resist economic risks than XY.

The correlation matrix of the four indicators is investigated to reveal their relationship, as shown in Fig. 13.

From Fig. 13, the indicators of P_{HSW} and B_{FG} show a strong negative correlation, and P_{VO} and N_M show a strong positive correlation. I_{RR} and P_{BP} are completely negatively correlated. B_{FG} is positive correlation with P_{BP} and strongly negative correlation with P_{VO} and N_M. N_M show positive correlation with P_{BP}.

Sensitivity analysis

The usage habit of a household's electricity is different, so a household's electricity consumption is probably not 10 kWh/day. Rural areas in some parts of Shaanxi Province in China may not suitable for such high-water heads, or the electricity price in Shaanxi Province may increase or decrease during the life cycle of the PV-PH system. Or would it
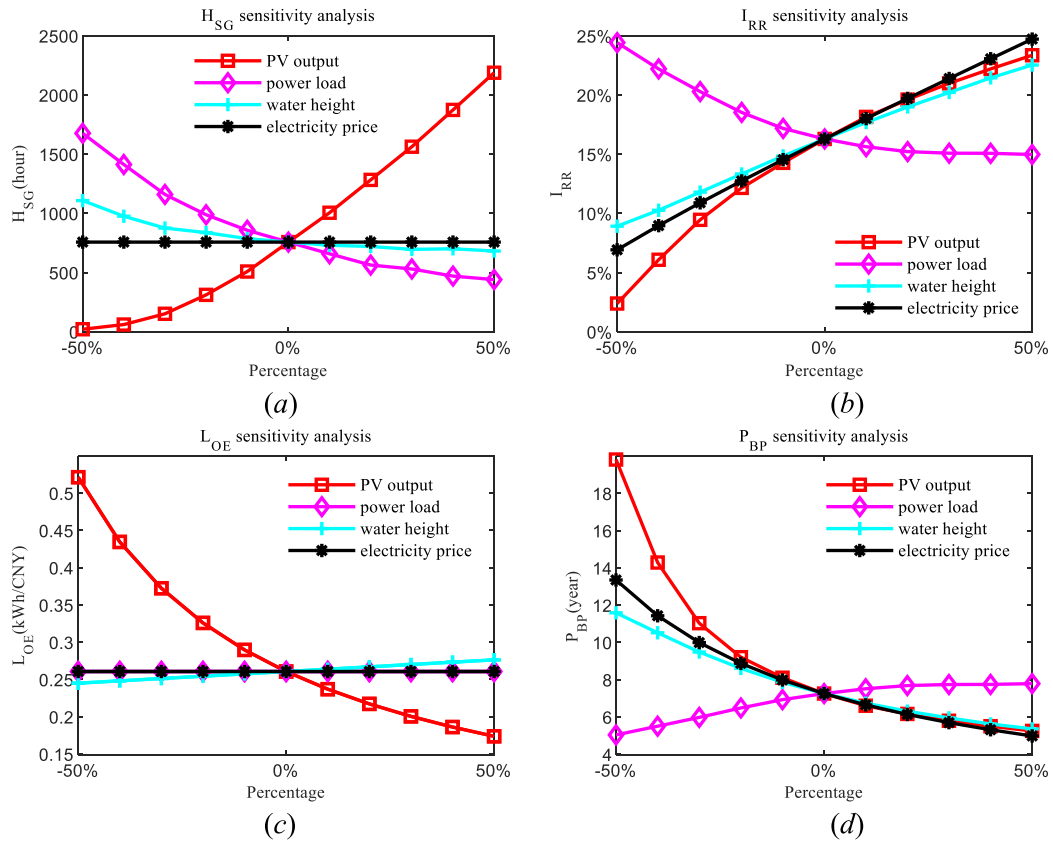
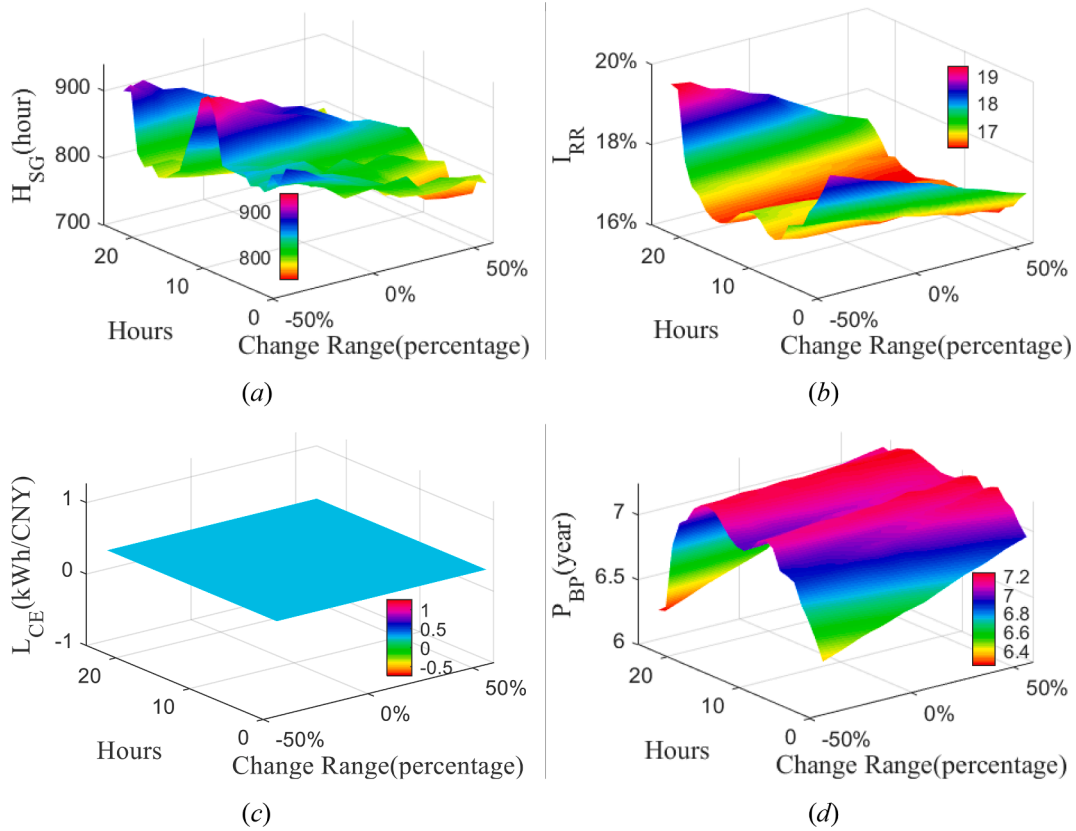**Fig. 5.** Family load characteristics of the load profile.

Fig. 6. Annual average solar irradiation and temperature of Shaanxi Province in China.

be better to wait a few years for solar photovoltaic panels to become more efficient and then promote this system? If so, how much revenue is added? Is it worth discarding these benefits and promoting the system right now? In this subsection, the sensitivity analysis is introduced to answer these questions. In this study, the sensitivity analysis of some core variables is analyzed. The selected core variables include the PV output, power load, water height, and electricity price. The output of the sensitivity results is selected as H_{SG}, I_{RR}, P_{BP}, L_{CE}. The sensitivity analysis results are shown in Fig. 14.

For the variable of power load, as shown in Fig. 14(a), it has a great impact on the indicators of H_{SG}, I_{RR} and P_{BP} expect L_{CE}. As shown in Fig. 14(b), it is worth noting that the increase of household power consumption cannot lead to a large increase of P_{BP}. While the household power consumption is reduced, it can significantly shorten P_{BP} to about five years, which is really an investment with a short payback time. Nevertheless, these two indicators still show good levels. As shown in Fig. 14(c), the sensitivity of the power load also shows a similar trend for I_{RR}. If the user's home power consumption increases, the I_{RR} cannot significantly reduce (about 15%); but if the user's home power consumption is reduced, it significantly increases the I_{RR} (about 25%). Fortunately, I_{RR} always far exceeds the bank's interest rate. It is meaning that this is a very worthwhile investment. As shown in Fig. 14(d), the increase of power load significantly reduces the value of H_{SG}, but the number of hours sold to the grid each year probably be more than 500 h.

For the output power of the PV-PH system, it has a significant impact on the indicators of H_{SG}, I_{RR} and P_{BP} and L_{CE}. Specifically, when the PV output changes from −50%to +50% of PV's rated power, the four indicators are more than three times as large as before. Therefore, if the household economy is poor, the return of investment could be better if the efficiency of the photovoltaic power generation increases after a few years.

For the water height of the surge tank, as shown in Fig. 14(a), it shows a small impact on L_{CE}. With the increase of head height, the indicator L_{CE} shows a very limited changes varying from 0.24 to 0.27. H_{SG} decreases with the increase of head height, and the range of variation is large, from 1100 to 680, as shown in Fig. 14(d). P_{BP} decreases as the height of the water head increases, and the minimum value reaches about five years, while I_{RR} increases as the height of the water head increase, up to 22%, as shown in Fig. 14(c) and (d) respectively.

Based on the above sensitivity analysis, the economic indicators of the PV-PH system are still within a reasonable and acceptable range even if the household power load changes. Therefore, the PV-PH system is suitable for popularization in Shaanxi Province. In its life cycle, the rise of electricity price helps to significantly improve the economic benefits for the household. The height of the water head has an impact on the economic indicators of the PV-PH system. Just like the change of electricity load, the change of economic indicators is still within a reasonable range under the boundary conditions in Shaanxi Province. In addition, the solar energy is quite sensitive to the changes of the four indicators. Therefore, consider the solar energy situation in this area should be considered and evaluated if the household are spreading it in other parts of China.

In addition, the habit of electricity consumption is different for households. Hence, the sensitivity performance of household electricity consumption is investigated, and the obtained results are shown in Fig. 15.

As shown in Fig. 15(a), increasing power consumption at night and noon is the fastest way to decrease H_{SG}. In the process of changing from −50% to +50%, H_{SG} dropped from 900 h to 800 h. But in the afternoon, increasing power consumption around 3o'clock and after 10o'clock has little effect on the changes in H_{SG}. As shown in Fig. 15(b), the increase of electricity consumption at night leads to a quickly drop of indicator I_{RR}, but the increase in electricity consumption during the day, especially around 9 am and 3 pm, cannot reduce the I_{RR} much. As shown in Fig. 15 (c), the change in power consumption has no effect on L_{OE}. As shown in Fig. 15(d), the less power consumption, the shorter P_{BP} value. Increasing

power consumption at night significantly increases the value of P_{BP}. But even if it increases by 50%, P_{BP} increases by about 1 year, and P_{BP} is still within the acceptable range.

Discussion and conclusion

In this study, the feasibility of a photovoltaic-pumped hydropower generating system is proved to be used in rural residential households with wells. The studied system in this research is focused to apply to Shaanxi Province in China. The genetic algorithm is used to optimize the number of photovoltaic arrays, the size of the water tank, and the height of the water head to find the suitable techno-economic performance of this system in different prefecture-level cities of Shaanxi Province. To achieve this goal, eight techno-economic indicators, including the hour sold to the grid (H_{SG}), the PV output (P_{VO}), the hours bought from the power grid (B_{FG}), the pumped capacity (P_{HSW}) (b) the internal rate of return (I_{RR}), the levelized cost of energy (L_{CE}), the payback period (P_{BP}), and the net margin (N_M). Four main conclusions are concluded. First, the range of P_{BP} in ten prefecture-level cities changes from 6.41 years to 8.14 years, and the range of N_M is from 314.2 CNY to 541.61 CNY. The range of H_{SG} is from 547.09 kWh to 1077.42 kWh, and the range of B_{FG} is from 953.00 kWh to 1690.00 kWh. Among the ten cities, the system in *Yulin*, *Yanan*, *Xianyang* and *Shangluo* have the best comprehensive performance from the eight major indicators. The system in *Weinan*, *Tongchuang*, and Baoji shows a better performance, while the system in *Ankang* and *Hanzhou* has the worst performance. Second, from the energy flow analysis, the system meets about 4/5 of the household's electric load, and the variables of the system have a significant impact on the household energy flow and load demand. Specifically,

(1) The change of household's load demand has no effect on L_{CE}, but it has a great impact on I_{RR}, P_{BP} and H_{SG}.
(2) When the power output of the photovoltaic panel changes from −50% to +50%, the four evaluation indicators (H_{SG}, P_{BP}, I_{RR} and L_{CE}) change more than three times. Therefore, this system is more suitable for promotion in places with more sufficient sunlight.
(3) The height of the water head has little impact on H_{SG}. It has a greater impact on the three indicators of P_{BP}, I_{RR} and L_{CE}, but this impact changes in an acceptable range in tech-economic performance. Therefore, this system still brings good economic benefits to the family even in some one-story rural families.
(4) The electricity price shows a low sensitive to indicators of L_{CE} and H_{SG}. However, the increase of electricity price rapidly shortens P_{BP} and increases I_{RR}. Therefore, the increased electric price brings a better economic benefit to households during the life cycle of the system.

In summary, the photovoltaic-pumped hydropower generating system is suitable used in rural residential buildings with wells, and it is suitable for promotion in rural areas of Shaanxi Province.

CRediT authorship contribution statement

Zongru Yang: Conceptualization, Methodology, Writing – original draft, Writing - review & editing. **Guoxiu Sun:** Software, Investigation, Data curation, Writing - review & editing. **Paul Behrens:** Investigation, Writing - review & editing. **Poul Alberg Østergaard:** Writing - review & editing. **Mònica Egusquiza:** Writing - review & editing. **Eduard Egusquiza:** Writing - review & editing, Supervision. **Beibei Xu:** Funding acquisition, Writing - review & editing. **Diyi Chen:** Funding acquisition, Supervision, Writing - review & editing. **Edoardo Patelli:** Supervision, Writing - review & editing.

Declaration of Competing Interest

The authors declare that they have no known competing financial

Appendix

SI 1 supplementary methods

The nomenclature used in the methods below are listed in Table 1.

Nomenclature			
PV-PH	The Photovoltaic-Pumped Hydropower Generating System		
PWSS	The Pump Water Storage System		
MCDM	The Multi-criteria Decision-Making method		
XA	*XiAn*	AK	*AnKang*
YL	*YuLin*	HZ	*HanZhong*
WN	*WeiNan*	BJ	*BaoJi*
YA	*YanAn*	TC	*TongChuang*
XY	*XianYang*	XA	*Xi'An*
SL	*ShangLuo*	YL	*YuLin*
h_0	The current height of the water tank		m
h_x	The water pump increases the height of the water in the water tank every time the water is pumped		m
h_s	The maximum amount of water that the pump can pump in one hour		m
h_1	Water tank height		m
W_0	Electric energy required for pumping h1-h0		kWh
h_3	E_0 corresponds to the height of falling water h_3		m
E_1	Electricity generated by the generator per hour		kWh
E_2	The electric energy that water at h_0 height can generate		kWh
S_{PP}	Solar photovoltaic panel		p.u.
G_A	Genetic Algorithm		p.u.
P_{BP}	The payback period		p.u.
I_{RR}	The internal rate of return		p.u.
L_{CE}	The Levelized Cost of Energy		p.u.
N_M	The net margin		p.u.
H_{SG}	The hours sold to grid		p.u.
P_{VO}	The PV output		p.u.
B_{FG}	The hours buy from to the grid		p.u.
P_{HSW}	The PHS pump water		p.u.

SI 1.1 modelling of solar array

The parameters of the PV array are listed in Table 1. The power output of a PV power generation unit depends on the solar irradiance, ambient temperature, and the PV panel characteristics. The I–V and P–V curve be plotted using the single-diode model of the solar cell. The relationship between I and V be expressed as follow:

$$I = I_{ph} - I_0\left(e^{\frac{V-IR_s}{V_t}} - 1\right) - \frac{V+IR_s}{Rl} \tag{6}$$

where I is the output current(A); I_{ph} is the photocurrent or short circuit(A); I_0 is diode reverse saturation currents(A) of the panel; R_s and R_p is the series resistance(Ω) and shunt/parallel resistances, respectively; $V_t = nKT/q$ is the thermal voltage(V); n is known as diode ideality factor; T is the cell temperature(K); K is Boltzmann's constant (1.381×10^{-23} J/K); q is the electron charge (1.602×10^{-19} C) (see Table 2).

According to the module's specification, the five key parameters I_{ph}, I_0, V_t, R_s, and R_p are calculated under standard test conditions (STC). Then, the parameters under general operating conditions simply are attained by considering the influences of solar radiation and PV cell temperature. Therefore, the power output of a PV model be expressed as:

$$P_{PV} = I_A V_A = N_P I_{ph} V_A - N_P I_0 V_A \left(e^{\frac{1}{V_t}\left(\frac{V_A}{N_S}+\frac{I_A}{N_P}R_s\right)} - 1\right) - \frac{N_P}{R_P}V_A\left(\frac{V_A}{N_S}+\frac{I_A}{N_P}R_S\right) \tag{7}$$

where N_S refers to the quantity of PV modules in series for the studied array and N_P refers to the number of PV cells in parallel.

This formula is applied to any number of solar cells in series (N_S), and hence it is not limited to one cell. Namely, if here exist N_M cells linked in series, and there exist N_C solar cells in series in each module, then

$$N_S = N_M \times N_C \tag{8}$$

The maximum power point tracking function (MPPT) is generally involved in the inverter. Therefore, according to the above formula, the total P-V curve and the maximum power value are obtained in this study.

SI 1.2 supplementary Shaanxi data

References

[1] Jinping Xi. Speech ——— Carrying on the past and opening up a new journey of global response to climate change. <http://www.gov.cn/gongbao/content/2020/content_5570055.htm?ivk_sa=1024320u>.

[2] Opinions on the implementation of photovoltaic power generation poverty alleviation work. <http://www.cpad.gov.cn/art/2016/3/25/art_46_56344.html>.

[3] Li Yi, Liu Y, Hu B, Li Yi, Dong J. Numerical investigation of a novel approach to coupling compressed air energy storage in aquifers with geothermal energy. Appl Energy 2020;279:115781.

[4] Guo C, Li C, Zhang K, Cai Z, Ma T, Maggi F, et al. The promise and challenges of utility-scale compressed air energy storage in aquifers. Appl Energy 2021;286:116513.

[5] He H, Du E, Zhang N, Kang C, Wang X. Enhancing the power grid flexibility with battery energy storage transportation and transmission switching. Appl Energy 2021;290:116692.

[6] Li J. Optimal sizing of grid-connected photovoltaic battery systems for residential houses in Australia. Renewable Energy 2019;136:1245–54.

[7] Thormann B, Puchbauer P, Kienberger T. Analyzing the suitability of flywheel energy storage systems for supplying high-power charging e-mobility use cases. J. Storage Mater. 2021;39:102615.

[8] Díaz-González F, Sumper A, Gomis-Bellmunt O, Bianchi FD. Energy management of flywheel-based energy storage device for wind power smoothing. Appl Energy 2013;110:207–19.

[9] Klimeš L, Charvát P, Mastani Joybari M, Zálešák M, Haghighat F, Panchabikesan K, et al. Computer modelling and experimental investigation of phase change hysteresis of PCMs: The state-of-the-art review. Appl Energy 2020;263:114572.

[10] Kong Y, Duan H, Egusquiza M, Beibei Xu, Chen D, Egusquiza E. Transient analysis to air chamber and orifice surge tanks in a hydroelectric generating system during the successive load rejection. Energy Convers Manage 2021. https://doi.org/10.1016/j.enconman.2021.114449.

[11] Ma T, Yang H, Zhang Y, Lu L, Wang X. Using phase change materials in photovoltaic systems for thermal regulation and electrical efficiency improvement: a review and outlook. Renewable Sustainable Energy Rev 2015;43:1273–84.

[12] Manfrida G, Secchi R. Seawater pumping as an electricity storage solution for photovoltaic energy systems. Energy 2014;69:470–84.

[13] Xu B, Chen D, Venkateshkumar M, Xiao Yu, Yue Y, Xing Y, et al. Modeling a pumped storage hydropower integrated to a hybrid power system with solar-wind power and its stability analysis. Appl Energy 2019;248:446–62.

[14] Li F-F, Qiu J. Multi-objective optimization for integrated hydro–photovoltaic power system. Appl Energy 2016;167:377–84.

[15] Yan J, Yang Y, Elia Campana P, He J. City-level analysis of subsidy-free solar photovoltaic electricity price, profits and grid parity in China. Nat Energy 2019;4(8):709–17.

[16] Ma T, Yang H, Lu L, Peng J. Pumped storage-based standalone photovoltaic power generation system: modeling and techno-economic optimization. Appl Energy 2015;137:649–59.

[17] Yu Y, Liu J, Wang Y, Xiang C, Zhou J. Practicality of using solar energy for cassava irrigation in the Guangxi Autonomous Region, China. Appl Energy 2018;230:31–41.

[18] Campana PE, Leduc S, Kim M, Olsson A, Zhang J, Liu J, et al. Suitable and optimal locations for implementing photovoltaic water pumping systems for grassland irrigation in China. Appl Energy 2017;185:1879–89.

[19] Lin S, Ma T, Shahzad Javed M. Prefeasibility study of a distributed photovoltaic system with pumped hydro storage for residential buildings. Energy Convers Manage 2020;222:113199.

[20] Kusakana K. Optimal operation scheduling of grid-connected PV with ground pumped hydro storage system for cost reduction in small farming activities. J Storage Mater 2018;16:133–8.

[21] Nfah EM, Ngundam JM. Feasibility of pico-hydro and photovoltaic hybrid power systems for remote villages in Cameroon. Renewable Energy 2009;34(6):1445–50.

[22] Pali BS, Vadhera S. A novel solar photovoltaic system with pumped-water storage for continuous power at constant voltage. Energy Convers Manage 2019;181:133–42.

[23] Anilkumar TT, Simon SP, Padhy NP. Residential electricity cost minimization model through open well-pico turbine pumped storage system. Appl Energy 2017;195:23–35.

[24] de Oliveira E, Silva G, Hendrick P. Pumped hydro energy storage in buildings. Appl Energy 2016;179:1242–50.

[25] Solar panel price <https://www.zhihu.com/question/382573204/answer/1780154196>.

[26] Household electric power data. <https://www.kaggle.com/winternguyen/predict-household-electric-power-using-lstm/notebook>.

[27] Campana PE, Li H, Yan J. Dynamic modelling of a PV pumping system with special consideration on water demand. Appl Energy 2013;112:635–45.

[28] Ebaid MSY, Qandil H, Hammad M. A unified approach for designing a photovoltaic solar system for the underground water pumping well-34 at Disi aquifer. Energy Convers Manage 2013;75:780–95.

[29] Hadj Arab A, Chenlo F, Benghanem M. Loss-of-load probability of photovoltaic water pumping systems. Sol Energy 2004;76(6):713–23.

[30] Bakelli Y, Hadj Arab A, Azoui B. Optimal sizing of photovoltaic pumping system with water tank storage using LPSP concept. Sol Energy 2011;85(2):288–94.

[31] Xiong Hualin, Beibei Xu, Kheav Kimleng, Luo Xingqi, Zhang Xingjin, et al. Multiscale power fluctuation evaluation of a hydro-wind-photovoltaic system. Renewable Energy 2021;175:153–66.

[32] Bouzidi B. New sizing method of PV water pumping systems. Sustainable Energy Technol Assess 2013;4:1–10.

[33] Stoppato A, Cavazzini G, Ardizzon G, Rossetti A. A PSO (particle swarm optimization)-based model for the optimal management of a small PV (Photovoltaic)-pump hydro energy storage in a rural dry area. Energy 2014;76:168–74.

[34] Carroquino J, Dufo-López R, Bernal-Agustín JL. Sizing of off-grid renewable energy systems for drip irrigation in Mediterranean crops. Renewable Energy 2015;76:566–74.

[35] Khoroshiltseva M, Slanzi D, Poli I. A Pareto-based multi-objective optimization algorithm to design energy-efficient shading devices. Appl Energy 2016;184:1400–10.

[36] Shaanxi Province Photovoltaic Subsidy Policy. <https://wenku.baidu.com/view/cd49fc977275a417866fb84ae45c3b3566ecdd68.html>.

[37] penstock price <https://detail.tmall.com/item.htm?spm=a230r.1.14.56.24dfd257loxq7q&id=614328589332&ns=1&abbucket=0>.

[38] Javed MS, Song A, Ma T. Techno-economic assessment of a stand-alone hybrid solar-wind-battery system for a remote island using genetic algorithm. Energy 2019;176:704–17.

[39] Digging well cost. <https://zhidao.baidu.com/question/373914389879097964.html>.

[40] Photovoltaic annual maintenance cost. <https://mp.weixin.qq.com/s/nSesjCS9qTHon-3AYkbIXA>.